EE

Internal Report
DESY M-94-03
July 1994

Reports at the European Particle Accelerator Conference EPAC'94

London, 27 June to 1 July, 1994

Studies of Measurement and Compensation Techniques of Magnet Motion for Linear Colliders

Chr. Montag, M. Lomperski, J. Rossbach
DESY
Notkestr. 85
D-22603 Hamburg

Abstract

To avoid loss of luminosity, most linear collider schemes require a very low mechanical jitter tolerance for the quadrupole magnets in the main linac. Typical values are an rms vertical vibration level below 40 nanometers for frequencies beyond 2 Hz (S-band linear colliders) or 5 nanometers for frequencies beyond 9 Hz (X-band), respectively. As these values are unlikely to be achieved in an active linac environment, some means of vibration damping will be necessary. The associated issues are being addressed as part of the DESY S-band Test Linac activities. Methods of measuring the motion of magnets, compensation techniques, and feedback algorithms are being investigated. The first results are presented here.

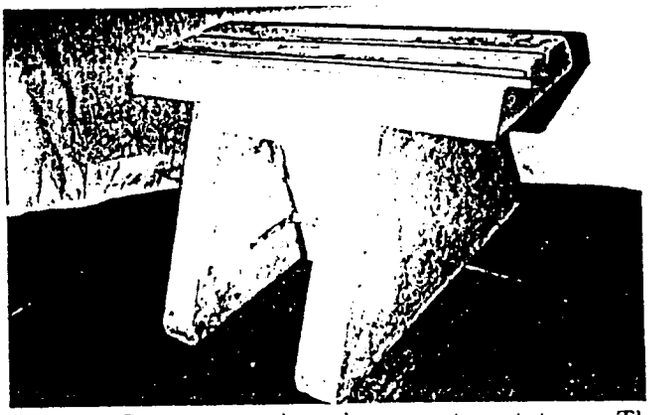

Figure 1: Concrete quadrupole support prototype. The ruler indicates 1 m.

1 INTRODUCTION

To achieve high luminosity of some $10^{33}\,\mathrm{cm}^{-2}\mathrm{s}^{-1}$ in a future linear collider which will be operated at a repetition rate of 50 Hz (e.g. DESY S-band [1]) to 150 Hz (JLC X-band), beam dimensions will have to be reduced to some 10 nanometers vertically and some 100 nanometers horizontally at the interaction point (IP). These beam dimensions require very low mechanical tolerances for the uncorrelated quadrupole jitter σ_q, which can be written as [2]:

$$\sigma_q = 0.25 \cdot \sqrt{\frac{\epsilon_y \overline{\beta}_{\mathrm{end}}}{N_q}} \cdot \cos\frac{\mu}{2}, \qquad (1)$$

where ϵ_y, $\overline{\beta}_{\mathrm{end}}$, N_q are the actual emittance at the end of the linac, the average β–function of the last FODO cell, and the total number of quadrupoles in the linac, respectively. μ is the (constant) phase advance per cell.
Since amplitudes of fast ground motion are 5 to 10 times larger than the vertical tolerances, it would be unlikely to collide the beams without using any correction method.
This paper describes different compensation schemes to overcome the problem of vertical ground motion acting on quadrupoles in linear colliders.

2 SUPPORT PHILOSOPHY

For compensation purposes, the spectrum of ground motion can be splitted into various frequency domains, each of them requiring different compensation schemes.
While for compensation of slow ground motion ($f \leq 0.05 \cdot f_{\mathrm{rep}}$) beam based orbit stabilization can be employed, a different method has to be considered for higher frequency components.

One considerable attempt to compensate fast ground motion consists of a passive damping system with a resonance frequency ω_0 well below 2 Hz (DESY S-band) which leads to an attenuation of vibration amplitudes proportional to ω^2 for frequencies $\omega \gg \omega_0$. This would result in vibration isolators with a quite small spring constant. Consequently, the compliance (i.e. the response to direct excitation of the support top) of such a system would be very large, and the absolute position would not be defined with sufficient accuracy. Therefore passive damping is applicable only in the high frequency range ($f > 100$ Hz).
To avoid excitation of inherent support resonances, it must be sure that no internal resonances below this limit are present. To achieve this, a very stiff support structure with high internal damping has to be designed. Together with the premise of low cost, an iron enforced concrete structure has been built.
To avoid amplification of ground motion in the horizontal direction, a high horizontal resonance frequency is necessary, which can be achieved by a triangular cross section of the support.
These considerations lead to the support design shown in figure 1.
For the compensation of fast ground motion in the 2 Hz to 100 Hz range, an active feedback system is under study. It consists of a highly sensitive motion sensor measuring mechanical vibration of each quadrupole and a piezoelectric actuator tilting the magnet around its transverse axis in order to keep its centre at rest. This is shown schematically in figure 2. Geophone type sensors applicable in such a feedback system have been successfully tested.

It is obvious that, once this scheme has been demon-

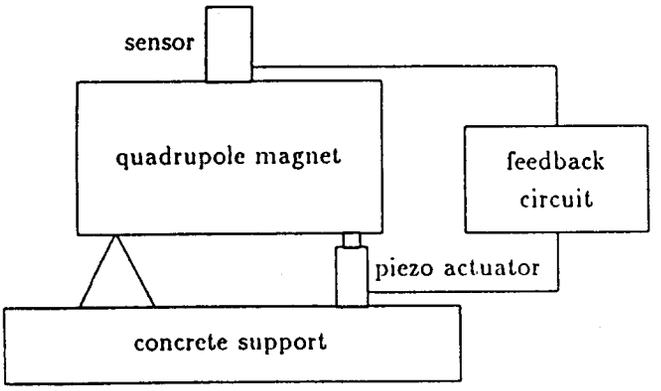

Figure 2: Schematic view of feedback system to compensate fast ground motion.

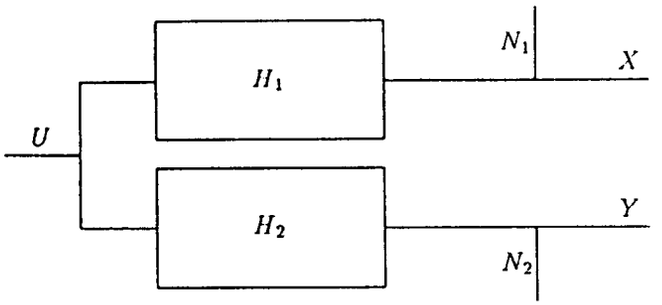

Figure 3: Two instruments with transfer functions H_1 and H_2 responding to the same signal $u(t)$. $U(s)$ is the Laplace transform of the input signal.

strated to work, one can alternatively consider correction dipole kicks instead of mechanical feedback.
To summarize this, the considerations mentioned above result in three frequency domains requiring different compensation techniques:

- $f < 2\,\mathrm{Hz}$ → beam based orbit stabilization,
- $2\,\mathrm{Hz} < f < 100\,\mathrm{Hz}$ → active mechanical stabilization,
- $f > 100\,\mathrm{Hz}$ → passive vibration absorption.

3 METHOD

The noise of various types of seismometers and the dynamical properties of the support structure have been measured. Due to the relatively large signals from ambient ground motion, two seismometers have been used, and an analysis of the coherence of their signals has been made. The method is described below, followed by the results.
Consider a general system shown in figure 3 consisting of two instruments, transfer functions H_1 and H_2, responding to the same input $u(t)$. The two outputs $x(t)$ and $y(t)$ consist of the input signal $u(t)$, transferred through the one or the other instrument, and a certain amount of noise ($n_1(t)$, $n_2(t)$) which is added to each of these ideal signals.
By using the Laplace-transformation, one can write these relations as

$$X(s) = H_1(s) \cdot U(s) + N_1(s) \quad (2)$$

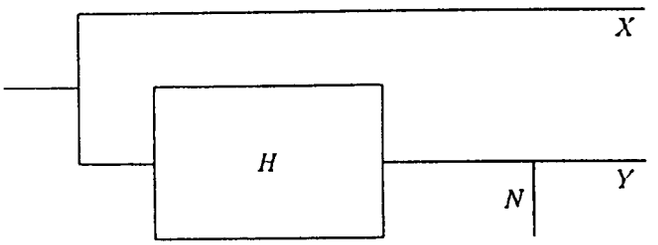

Figure 4: Equivalent model for coherence study.

$$Y(s) = H_2(s) \cdot U(s) + N_2(s), \quad (3)$$

where $X(s)$ is the Laplace-transform of $x(t)$, etc. $H_1(s)$ and $H_2(s)$ are the transfer functions of the one or the other instrument, respectively.
This can be rewritten as

$$Y(s) = H(s) \cdot X(s) + N(s), \quad (4)$$

with $H(s) = H_2(s)/H_1(s)$ and $N(s) = N_2(s) - H(s) \cdot N_1(s)$. This is shown schematically in figure 4.
The coherence function γ^2 is defined as [4]

$$\gamma^2 = \frac{|\Phi_{xy}|^2}{\Phi_{xx}\Phi_{yy}}, \quad (5)$$

with

$$\Phi_{xx} = X(\omega) \cdot X^*(\omega), \quad (6)$$
$$\Phi_{yy} = Y(\omega) \cdot Y^*(\omega), \quad (7)$$
$$\Phi_{xy} = X(\omega) \cdot Y^*(\omega), \quad (8)$$

where $X(\omega)$ is the Fourier-transform of $x(t)$, etc.
Since $\gamma^2 = 1$ for a single measurement, one has to take into account the average spectra of many measurements. For this reason each time series has to be divided into overlapping segments, the optimum overlap being 62.5% [5]. Then these segments are Fourier-transformed using a Hanning window and averaged over all spectra obtained from the various time signal segments.
Utilizing the averaged power spectra $\overline{\Phi}_{xx}$, $\overline{\Phi}_{yy}$ and $\overline{\Phi}_{xy}$, one gets the following relations:

$$H = \frac{\overline{\Phi}_{xy}}{\overline{\Phi}_{xx}}, \quad (9)$$
$$\overline{\Phi}_{nn} = \overline{\Phi}_{yy} - |H|^2\overline{\Phi}_{xx}, \quad (10)$$
$$\overline{\Phi}_{ss} = \overline{\Phi}_{yy} \cdot \gamma^2, \quad (11)$$
$$\beta = \frac{\overline{\Phi}_{xx}|H|^2}{\overline{\Phi}_{nn}} \quad (12)$$
$$= \frac{\gamma^2}{1-\gamma^2}, \quad (13)$$

where Φ_{nn}, Φ_{ss}, β are the noise power spectrum, signal power spectrum, and the signal-to-noise ratio, respectively.

4 RESULTS

Geophone type motion sensors manufactured by KEBE Scientific Instruments have been used in the tests. A Bode

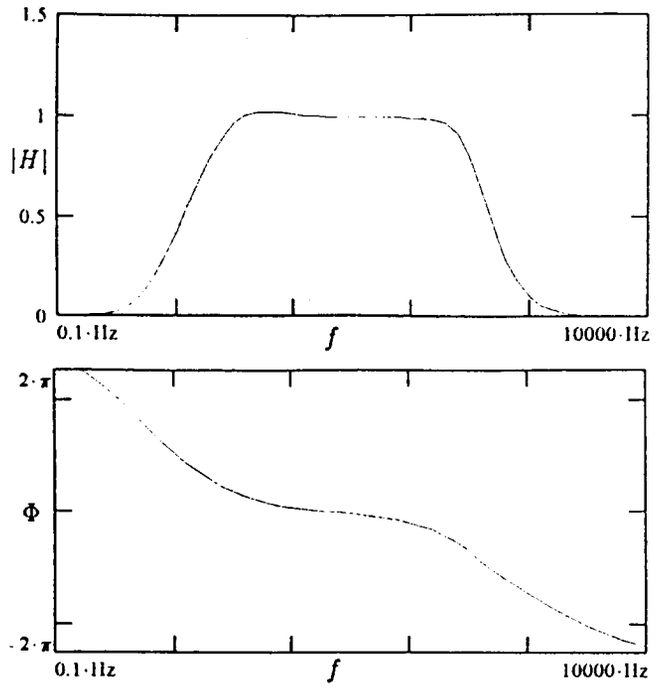

Figure 5: Bode plot of the transfer function of the KEBE geophone plus preamplifier.

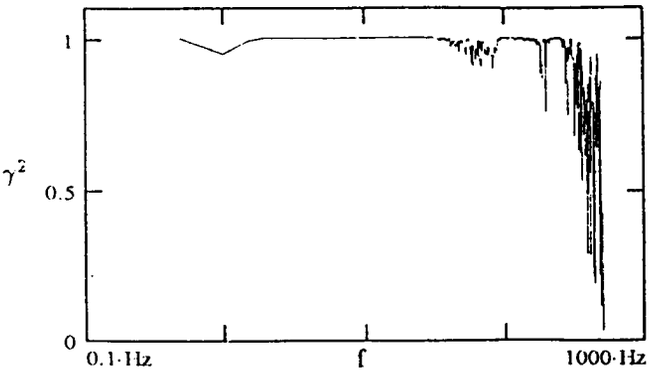

Figure 6: Coherence function γ^2 of two KEBE geophones placed side-by-side.

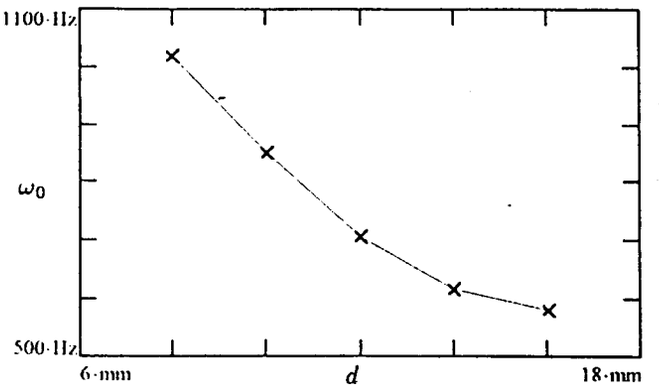

Figure 7: Measured mechanical resonance frequency ω_0 versus rubber thickness d.

plot of the transfer function of the geophone plus preamplifier is given in figure 5.

Each coherence function was obtained by averaging over 20 spectra sampled at 1 kHz, each segment consisting of 2048 data.

The noise of the KEBE seismometers has been obtained from the measurement of the coherence of two seismometers placed side-by-side. The relative transfer function, H, is expected to be 1, and the rms noise is given by the function $\overline{\Phi}_{nn}$.

Figure 6 shows the coherence function γ^2 of two geophones placed side-by-side. As seen in the picture, the outputs of the two geophones are nearly perfectly correlated in the 1 Hz to 300 Hz range, which corresponds to a large signal-to-noise ratio β (eq. 13). The rms noise in this frequency range, given by the integral of Φ_{nn}, is approximately 1.1 nm, which is well below the quadrupole jitter tolerance. Therefore these sensors might be applicable for feedback purposes.

The transfer function of the prototype support has been determined from the coherence function of two seismometers, one placed on top of the support and the second on the ground. This support (weight 260 kg) was placed on four rubber feet of a total area of 60 cm^2. The resonance frequency of the whole system (support plus rubber feet) was determined by measuring the complex transfer function H (Eq. 9) with one sensor placed on the ground, the other on top of the support. Figure 7 shows the measured resonance frequencies for different rubber feet thicknesses, the rubber area being 60 cm^2.

5 REFERENCES

[1] N. Holtkamp et al., Status of the S-Band Linear Collider Study, DESY M-93-05

[2] T. O. Raubenheimer, SLAC-Report-387, 1991

[3] S. D. Stearns, Applications of the Coherence Function in Comparing Seismometers, preprint, Albuquerque 1979

[4] S. D. Stearns, Digital Signal Analysis, Hayden, 1975

[5] G. C. Carter et al., Estimation of the Magnitude-Squared Coherence Function via Overlapped Fast Fourier Transform Processing, IEEE Trans. AU-21, No. 4, August 1973

[6] KEBE Scientific Instruments, Schwingungsmesser SMK-1, manual, Halstenbek 1994